Hindawi
International Journal of Antennas and Propagation
Volume 2023, Article ID 8723069, 12 pages
https://doi.org/10.1155/2023/8723069

Research Article

Performance Analysis of an *F*-Shaped Antenna for Wireless Applications

A. Gokula Chandar,[1] S. Kannadhasan,[2] R. Nagarajan,[3] Parameswari Subbian,[4] and Mahtab Mashuq Tonmoy[5]

[1]*Department of Electronics and Communication Engineering, Sri Venkatesa Perumal College of Engineering and Technology, Cherlopalle, Andhrapradesh, India*
[2]*Department of Electronics and Communication Engineering, Study World College of Engineering, Coimbatore, India*
[3]*Department of Electrical and Electronics Engineering, Gnanamani College of Technology, Namakkal, India*
[4]*Department of Electronics and Communication Engineering, Sairam Institute of Technology, Chennai, India*
[5]*Department of Computer Science and Engineering, Daffodil International University, Dhaka 1207, Bangladesh*

Correspondence should be addressed to Mahtab Mashuq Tonmoy; mahtab2598@diu.edu.bd

Received 22 November 2022; Revised 13 January 2023; Accepted 27 January 2023; Published 13 March 2023

Academic Editor: Flaminio Ferrara

The wide-band circularly polarised (CP) monopole antenna structure described in this article combines a defective ground plane with an *f*-shaped radiating monopole that is intended for impedance bandwidth and high axial ratio bandwidth (IBW). The faulty ground structure is etched as twin rectangular slots, an *F*-shaped slot, and a square slot with a corner cut off. The proposed antenna is $25 \times 25 \times 1.6\ \text{mm}^3$ in total. The prototype of the optimised antenna's far-field characteristics has been constructed, modelled, and experimentally confirmed. The simulated and measured return loss values are 3.19 to 7.4 GHz, with −32.48 dB and −38.42 dB, respectively. Axial ratio values are 4.37 to 7.22 GHz and 4.52 to 7.15 GHz, with an efficiency of 49.18% and 45.07%, respectively, for the simulated and observed bands. Gain levels in the whole CP band range from 2.8 to 3.3 dB. A continuous radiation efficiency of more than 90% is realised in the CP band. The suggested CP antenna has constant radiation qualities and is suitable for WLAN and WiMAX applications.

1. Introduction

A planar antenna is a popular choice among radiating components for effective transmission owing to its many benefits, including low manufacturing costs, small size, exceptional flexibility, and simplicity of design [1–3]. Circularly polarised antennas provide a variety of advantages over linearly polarised antennas, including reduced multipath interference and a decrease in polarisation mismatch [4–6]. To create a broad CP band, several techniques were recorded. Two rectangular horizontal slots in the ground plane may accommodate a modified rectangular monopole [7]. Two connected slots and an *F*-shaped feed are used [8, 9], as is an antenna assembly with a parasitic structure that protrudes [10, 11]. Two related elliptical slots were used [12–15]. An inverted "*L*" structure [16], a ring-shaped patch [17], a hook-shaped radiating patch [18], a rectangular patch with slots and an enhanced ground plane, and a patch with slots all provided good CP characteristics.

In this study, a broadband CP is shown using an *F*-shaped monopole antenna and two asymmetrical rectangular ground plane slots. A coplanar waveguide (CPW) supplies it with energy. Broad IBW and ARBW were obtained with the inclusion of a *T*-shaped slot and a square slot with a truncated corner. With dimensions of $25 \times 25 \times 1.6$ mm, the antenna is compact. 3. 3.19 to 7.4 GHz and 3.19 to 7.23 GHz, respectively, are the computed and observed return loss values 4.37–7.22 GHz and 4.52–7.15 GHz, respectively, were the observed and modelled CP bandwidths. Over the whole band, the constant gain

ranges from 2.8 to 3.3 dB. At 5.16 GHz, 95% radiation efficiency is the highest. The next parts go into the design process, the CP mechanism, and the analysis of the results. The past 10 years, in particular, have seen a large and swift advancement in wireless communications in the modern period. Personal communication device development will soon strive to give voice, data, image, DMB (Digital Multimedia Broadcasting), and video communications everywhere on the planet at any time with the aid of WLANs (wireless local area networks). The fast development of various WLAN protocols has created a need for small multiband antennas that operate in the right frequency bands for mobile WiMAX (IEEE 802.16e-2005 standard) and Wi-Fi (IEEE 802.11 standard) applications.

Wi-Fi operates in the 5 GHz range and the 2.4 GHz band (2.4 GHz–2.5 GHz) (5.15–5.35 GHz, 5.47–5.725 GHz, and 5.725–5.875 GHz). Mobile WiMAX operates on three frequencies: 3.5 GHz, 2.5 GHz, and 2.3 GHz (2.3–2.4 GHz) (3.4–3.6 GHz). Certain low-profile microstrip and printed slot antennas are considered to be required for Wi-Fi and mobile WiMAX operations. These antennas are able to overcome restrictions in size, weight, price, effectiveness, installation difficulty, and aerodynamic profile. The best choice to adhere to the aforementioned limits is an inverted-L antenna. This paper proposes a dual-band, two-element inverted-L antenna with appropriate numerical analysis for 3.5 GHz mobile WiMAX and 5 GHz Wi-Fi operation with acceptable return loss, gain, and VSWR. We investigated the potential for streamlining the design of the dual-band flat-plate antenna with a shorted parasitic element for 2.4 and 5.2/5.8 GHz operations, and we designed the antenna not only for Wi-Fi operation but also for mobile WiMAX operation. A 50 ohm coaxial cable is projected to be used to feed this modified antenna, with the cable's outer conductor being connected to the ground plane and its inner conductor being connected to the feeding point. The recommended antenna is small enough to fit in mobile WiMAX and Wi-Fi networks and has compact dimensions for connectivity.

The *E*-shaped patch antenna is much simpler to design than the U-slot microstrip patch antenna. The dielectric sheet is placed on a ground plane, and the *E*-shaped patch is positioned on its highest point. The wireless sensor network (WSN) consists of geographically scattered autonomous sensors that monitor environmental or physical conditions, such as temperature, sound, vibration, weight, movement, or toxins, and chivalrously transmit their data to an important location. These days, similar systems are used in a variety of mechanical and consumer applications, including home computerization, social insurance applications, machine health monitoring, and contemporary process observation and control. Microstrip patch antennas are of considerable interest because of their positions of safety, light weight, satisfaction to planar and nonplanar surfaces, ease and cheapness to develop by way of advanced printed circuit technology, mechanical robustness when mounted on unbending surfaces, comparable with MMIC outlines, and growing requirements in wireless correspondence framework applications. When a certain shape and mode are chosen, they provide versatility with respect to their frequency, polarisation, example, and impedance [19–25].

As antenna technology develops daily, compact antennas that work well are in great demand. The wider bandwidth and gain of many conventional antenna structures, such as the Yagi, Parabolic Reflector, Helical, and Horn, among others, are constrained by their large size, which prevents their use in a variety of applications. As a result, these antennas cannot be used in devices that are smaller in size and are used to move an object. Microstrip antennas are often employed to fulfil this need for wireless communication, which fits the needs of the wireless communication system.

Return loss measures how well electricity is delivered from a transmission line to a load, such as an antenna. If there is a discrepancy between the power incident on the antenna-under-test (AUT) and the power reflected back to the source, the ratio may be used to calculate the degree of the mismatch. The better the match between the load and line, the greater this power ratio is. The load and line match up better when this power ratio is higher. Difference between how much power is sent to the AUT and how much power is shown in decibels. It is a positive, nondissipative phrase that describes how much the amplitude of the reflected wave is reduced in relation to the incident wave. A passive AUT should be used in this scenario. In other words, return loss is the reflection coefficient's decibel equivalent of the negative sign regarding the voltage-to-standing-wave ratio.

When a transmission system discontinues, the power consequent upon the discontinuity differs. (B) The difference in decibels between the power that hits the discontinuity and the power that bounces off of it. Notably, this ratio is also equal to the square root of the magnitude of the reflection coefficient. (C) In a broader sense, the return loss is a measurement of the difference in impedance between two objects, being equal to the number of decibels that is equal to the scalar value of the reciprocal of the reflection coefficient. Although its application in microwaves and antennas is connected to the development of the Smith chart, the notion of return loss has a murky history. When referring to reflection and mismatch in the present, return loss is the most often used word.

The phrase is commonly confused, however, with a reflection coefficient that has been given in decibels (dB). The reflection coefficient's magnitude is logarithmized; however, this is wrongly referred to as return loss. The outcome is still the reflection coefficient, but expressed in decibels. I originally questioned if a common textbook or software programme used the erroneous concept when thinking about the issue of return loss usage, but I couldn't find any support for this supposition. Now, writers are notified as soon as feasible before acceptance. The proper use of technical words is essential for ensuring uniformity and averting misunderstandings more widely and beyond return loss [26].

The microstrip patch antenna has recently been used in wireless communications applications, including radar, space communication, satellite communication, microwave communication, and mobile communication, among others [27–29] because of its inexpensiveness, ease of integration

with microwave integrated circuits, low volume, low-profile planar designs, and light weight. Due to its benefits, communications have focused on microstrip patch antennas during the last 20 years. Narrow bandwidth, surface wave excitation, limited gain, and a depleted radiation pattern are further drawbacks of the microstrip patch antenna. To address the drawbacks of patch antennas, intensifier research has been done. To boost the bandwidth and get around the restrictions, many strategies using variously shaped patch antennas are used. Due to their superior mechanical and electrical properties, ability to be integrated with other RF systems, and ability to be produced in large quantities, printed patch antennas are appropriate for wideband applications. This article looks into the specific absorption rate (SAR) of a planar inverted-F antenna (PIFA) with a rectangle shape at a frequency of 2.6 GHz [26]. Please rephrase the sentence for clarity. The Minkowski prefractal PIFA's resonant frequency may be adjusted by varying the size of the rectangular cutouts, while the square PIFA resonates at around 2.7 GHz. This results in the first variation, which has a cut-out dimension of 4 mm by 4 mm and demonstrates a resonant frequency of 2.36 GHz.

2. Design of *F*-Shaped Antenna

The design was composed of two layers, the first of which had an *F*-slot and the second of which had an *F*-shaped patch. The proposed antenna worked with both WLAN (2.4 GHz) and WiMAX (3.5 GHz). The main objective of the next generation of wireless communication systems is high-speed networking for multimedia communication. Microstrip antennas are interesting to many microwave and wireless communication systems owing to their many advantages, such as their small weight, simplicity of manufacture, cheap cost, etc.; yet, due to their confined input impedance and bandwidth, they are not employed in modern microwave systems. An antenna's miniaturisation, expanded bandwidth, high input impedance, and gain effectiveness are its primary performance criteria. Due to the rapidly increasing demand for wireless broadband communications, wireless local area networks (WLANs: 5.150 GHz–5.350 GHz) now need to provide quality of service, security, handover, and higher throughput. This band may be obtained in a tiny system using the DGS method. The advantages of DGS are analysed in terms of how quickly designers can produce a variety of wireless devices, which is not possible with the usage of conventional applications. In a two-element microstrip array, surface waves are suppressed by a DGS unit, leading to very high isolation between array elements. The flaw in the ground is one of the unusual ways to decrease antenna size, increase bandwidth, and hence improve antenna performance. A DGS feature known as dual band gaps offers a high-order matching network for capacity augmentation. As a consequence, for a given frequency, the antenna size is smaller when constructing an antenna using the defective ground construction technique than it would be without the ground defect. A shape defect on a ground plane may impede the dispersion of the insulated current depending on its shape and size. The disturbance at the shielded current distribution will have an impact on the input impedance and current flow of the antenna. The electromagnetic waves that are moving through the substrate layer may also be controlled by it. This technique is more cost-effective since it just requires one antenna to operate a certain design rather than numerous antennas. A rectangular microstrip line-fed patch antenna with a problematic ground design is shown in this article.

The objective is to develop a wideband microstrip antenna that can function over a broad frequency range. Broadband antennas served as inspiration for the design idea. The rectangular shape and faulty ground construction technique are both used because of the high input impedance. It was thus only possible to reduce the size of the patch and consequently the size of the microstrip antenna with higher bandwidth by using a flawed ground construction. A two-layer substrate antenna has been used in this design to provide multiband functioning for a range of wireless applications that cover the upper band of WLAN applications using microstrip feeding technology. The main elements of the proposed antenna design are a rectangular patch with an *E*-shaped slot and an *H*-shaped defect with a corner extending into the ground plane. A parametric study is carried out to understand the recommended antenna's characteristics.

A typical kind of radio antenna called a monopole has an *L*-shaped ground and a straight wire that rises perpendicular to it. It uses a half-dipole antenna, which consists of two identical rods, to transmit signals. The wavelength of the antenna affects the maximum power it can generate. There are several common forms of monopole antennas, such as ground plane antennas, *F*-antennas, and *L*-shaped slits. In this project, we are using an *F*-shaped slit and an *F*-antenna connected to a ground plane for WIMAX, ISM, and *C*-band applications. These antennas have developed into inverted antennas, which are used more often in internet networks and mobile applications. This monopole's design made use of the Fr-4 substrate. There have also been reports of other radiation types. The asymmetric ground is largely responsible for enabling the monopole antenna, which is used to transmit power to the antenna and enhance isolation. The flat shape is odd given the uneven surroundings. Due to the similarity of the antenna components, $S11 = S22$ and $S12 = S21$. These monopole antennas need a large ground plane, such as a square, rectangle, or ellipse. The performance of the antenna is influenced by the ground plane. A *T*-shaped antenna is buried in the earth to allow the lower frequency to descend with a cut-off frequency. The radiation qualities have also been improved by the asymmetric ground. The monopole antenna may be used with isolation of less than −22 dB, which is a very low number. As it can broadcast across great distances for a bigger user base, WiMax may operate similarly to Wi-Fi. WiMax is 802.16, just as Wi-Fi is 802.11.

As illustrated in Figure 1, the proposed design calls for an *F*-shaped monopole antenna with slots on the ground plane and a CPW line feeding it for circular polarisation with wide

IBW and ARBW. An FR4 dielectric substrate with gb, gc, and a height of 1.6 mm is used to build the antenna. As shown in Figure 1, a *T*-type slot with dimensions sa-sf, a corner-truncated square slot with dimensions gn-gr, another slot with dimensions gd-gm and gs-gu, and an in-ground plane are all employed to boost the antenna's axial ratio bandwidth. Table 1 is a list of the lengths.

Figure 2 displays the recommended antenna's *S*11 and axial ratio. IBW has a bandwidth of 4.04 GHz and operates between 3.19 and 7.23 GHz. The CPband's 2.85 GHz bandwidth spans the frequencies of 4.37 GHz and 7.22 GHz. In Figure 3, the VSWR and the gain plot are shown. VSWR operates between the frequencies of 3.19 GHz and 7.23 GHz. The gain, which is always 3 dB and covers the whole allowable spectrum for circular polarisation, is shown in Figure 3. Figure 4 displays the surface current distribution at 4.75 GHz and 7.05 GHz. For circular polarisation, it covers the whole WLAN 5.8 GHz and WiMAX 5.5 GHz spectrum.

3. Circular Polarization Mechanism

Figures 5–7 depict the CP radiation process at frequencies of 4.71 GHz, 5.7 GHz, and 7.05 GHz, respectively. CP may be identified by analysing the electric field distribution at various points in phases 00, 900, 1800, and 2700. Because the surface current rotates clockwise when seen from the +*z*-direction, LHCP radiation is generated at all frequencies.

4. Results and Discussion

Prior to construction, the suggested antenna was simulated with the ideal dimensions, as shown in Figure 8 with an example. Figure 9 displays measured reflection coefficients as well as VSWR pictures. Figure 10 compares the estimated and actual values for return loss and axial ratio. The measured return loss bandwidths range from 3.19 to 7.4 GHz and are 79.5% wide. The measured CP bandwidths are 45.07 percent and span the frequency range of 4.52 to 7.15 GHz. There is compatibility for all WLAN and WiMAX frequencies.

WLAN, UWB, and RFID applications benefit greatly from the use of small printed monopole antennas. The antenna should preferably be affordable, light in weight, less brittle, and low-profile, in addition to being compact. Furthermore, the production procedure must be simple. There are various tiny printed monopole antennas for wireless applications that have been developed, according to the literature.

Publications also display antennas based on the metamaterial approach for WLAN and WiMAX applications. For WLAN and WiMAX applications, complementary split ring resonators (CSRRs) were utilised in the radiator of a tiny antenna to block the 3.4, 4.1, 4.8, and 5.6 GHz bands. Ken also offered the general proportions of a broadband antenna consisting of two radiator elements and two interspaced ring resonators printed on an FR-4 substrate.

The antenna offered two bands of about 0.7 and 1.3 GHz at 2.4 and 5.8 GHz. With a CPW-fed metamaterial antenna, it was proposed to allow WLAN and WiMAX applications in

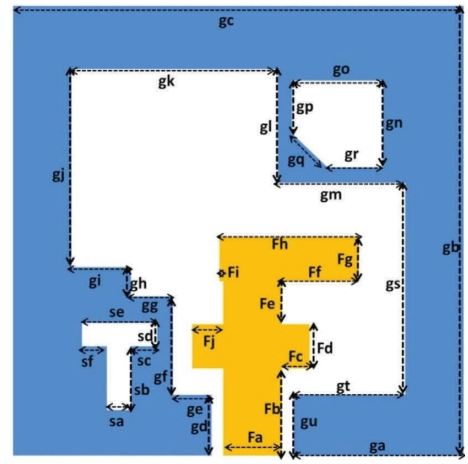

Figure 1: Antenna geometry.

Table 1: Design parameters of the proposed antenna.

Parameter	Units (mm)
Fa	2.6
Fb	3.8
Fc	1.4
Fd	2
Fe	2.2
Ff	4.2
Fg	2
Fh	7
Fi	0.2
Fj	1.4
4.32–7.32 GHz	
Ga	9.9
Gb	23
Gc	23
Gd	3.2
Ge	2
Gf	3.85
Gg	2.05
Gh	1.05
Gi	2.85
Gj	12.1
4.32–7.32 GHz	
Gk	10.1
Gl	6.9
Gm	6.9
Gn	5.25
Go	5.25
Gp	3.25
Gq	2.83
Gr	3.25
Gs	10.1
Gt	6.9
4.32–7.32 GHz	
Gu	3.2
Sa	1
Sb	2.5
Sc	1
Sd	1
Se	2.75
Sf	0.75

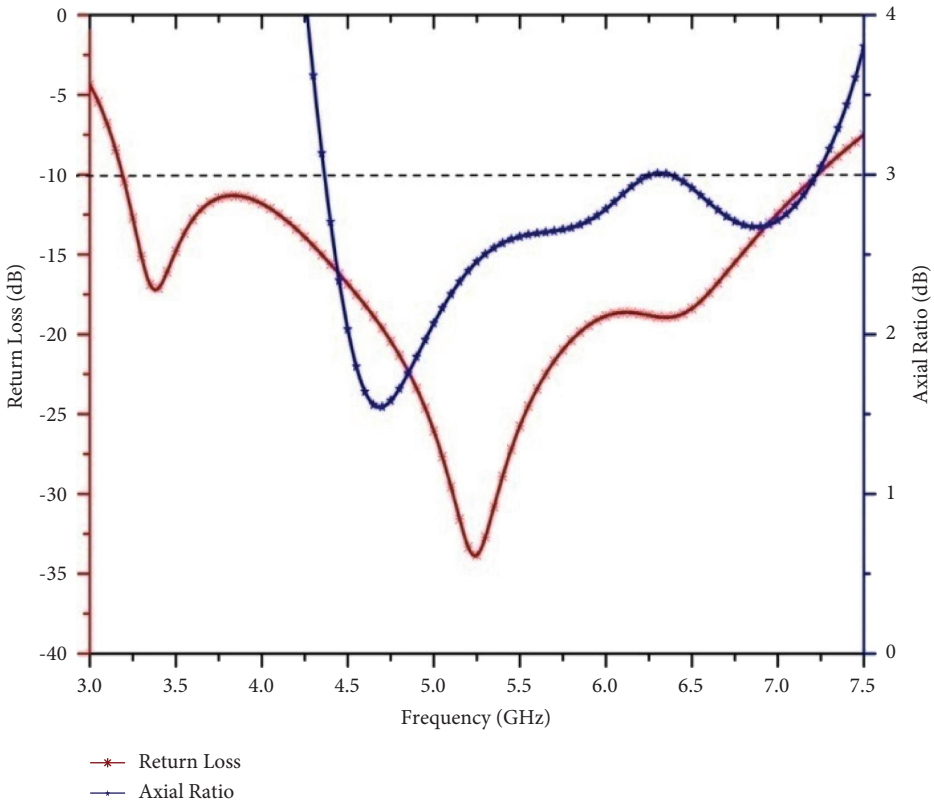

Figure 2: Return loss and axial ratio.

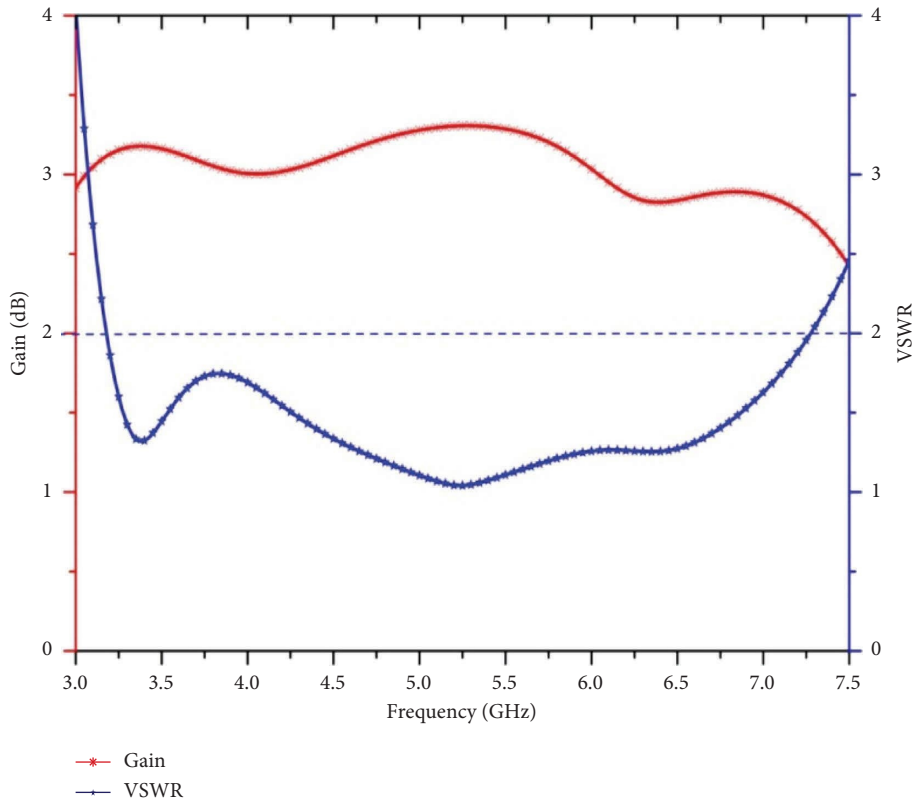

Figure 3: Gain and VSWR.

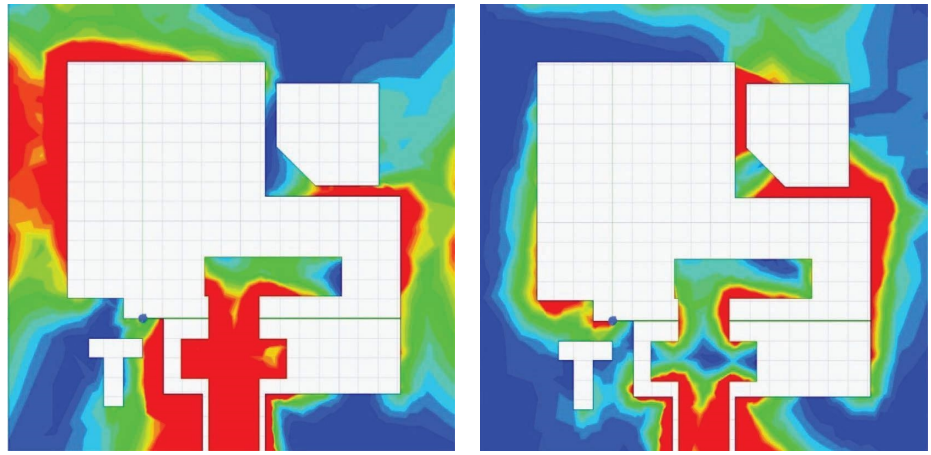

(a) (b)

Figure 4: Current distribution at (a) 4.75 GHz and (b) 7.05 GHz.

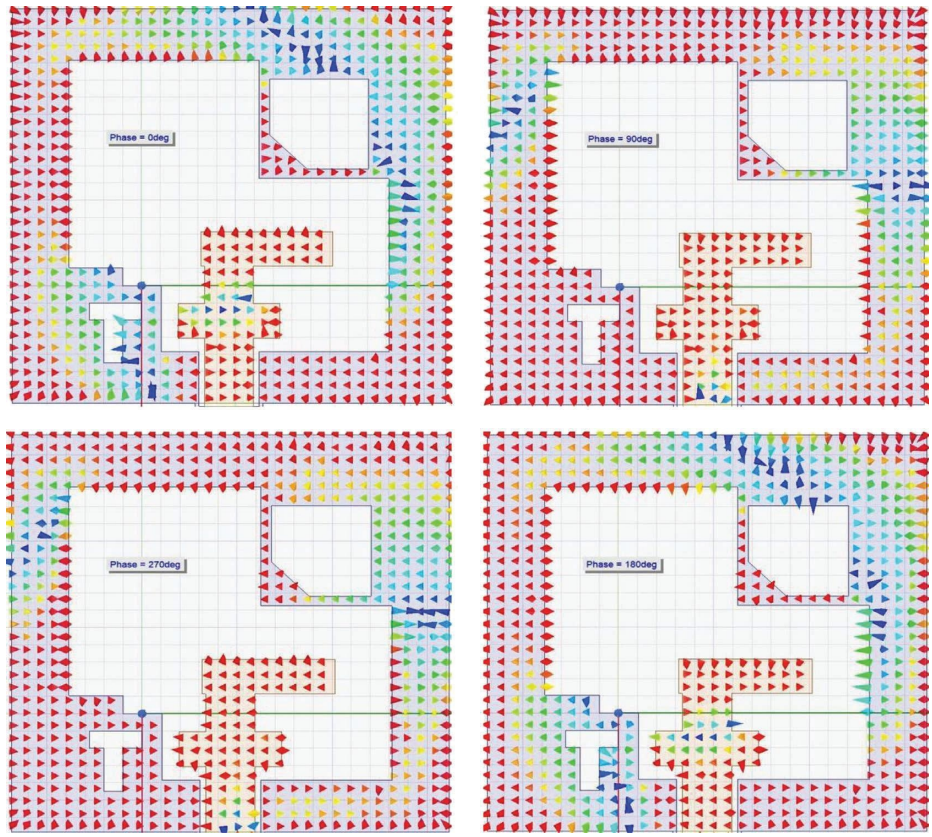

Figure 5: Circular polarization at 4.71 GHz.

the 2.4/5.5 GHz and 3.5 GHz bands, respectively. The MIMO antenna developed by the researchers consists of two spider-shaped radiators printed on an FR-4 substrate and is intended to block WLAN and WiMAX frequencies.

A model of a MIMO antenna with dual operating bands was constructed using four components, which were placed on each side of the dielectric material. Each piece has a rectangular open-loop resonator inserted into its ground plane. The bandwidths of the antenna were 0.08 GHz and 0.17 GHz at 2.46 GHz and 3.5 GHz, respectively. WLAN (2.4–2.485 GHz) and WiMAX (3.4–3.6 GHz) bandwidth requirements were met.

Based on the aforementioned numerical evaluation, the recommended antenna seems to be a solid option for mobile WiMAX and Wi-Fi operations. Due to its low profile, the proposed antenna may potentially be included in wireless devices utilising Wi-Fi and mobile WiMAX applications. Our long-term objective is to reduce the size of the proposed

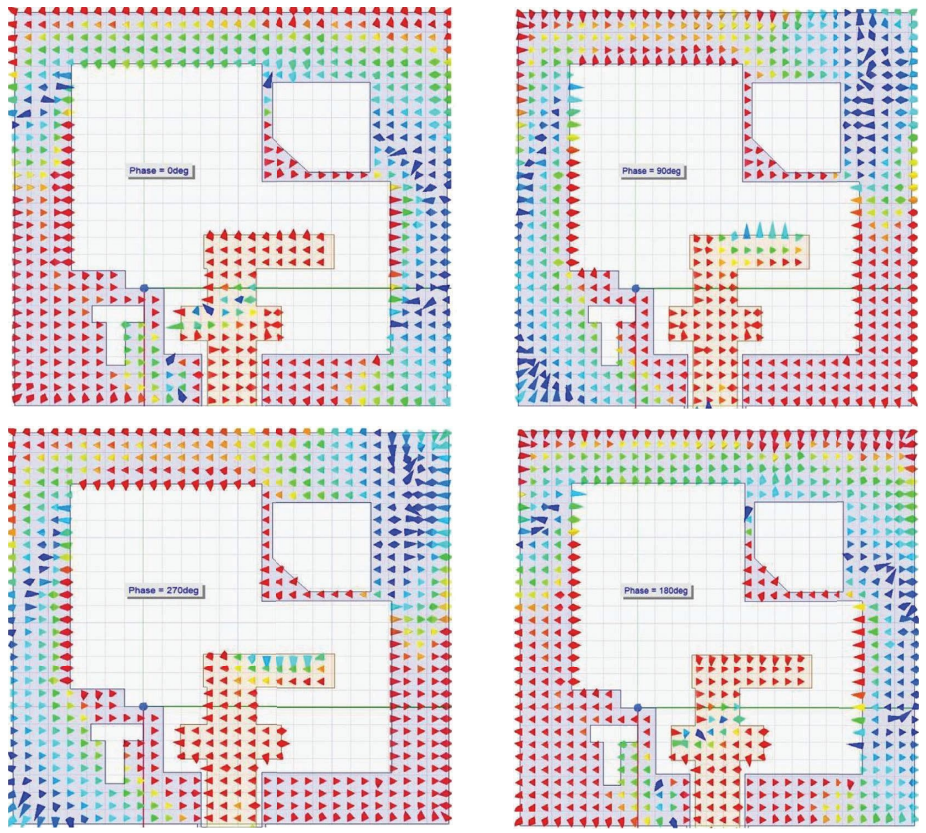

Figure 6: Circular polarization at 5.7 GHz.

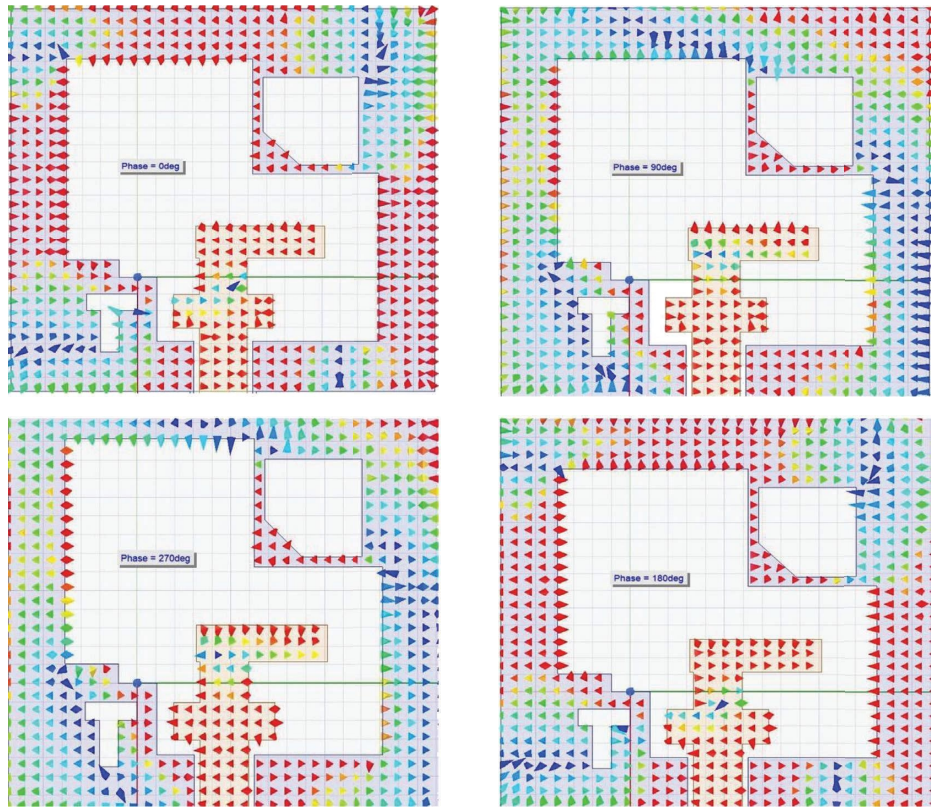

Figure 7: Circular polarization at 7.05 GHz.

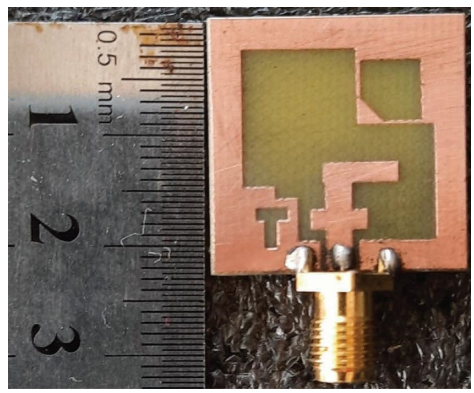

Figure 8: Fabricated antenna.

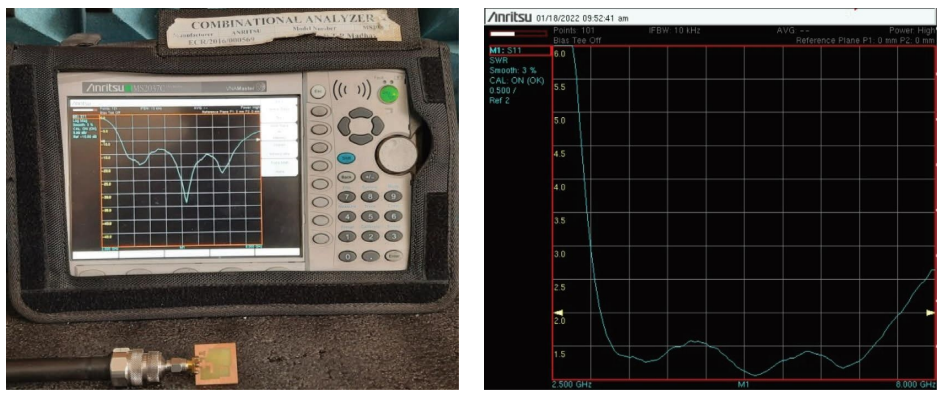

(a) (b)

Figure 9: Fabricated antenna measurement of (a) return loss and (b) VSWR.

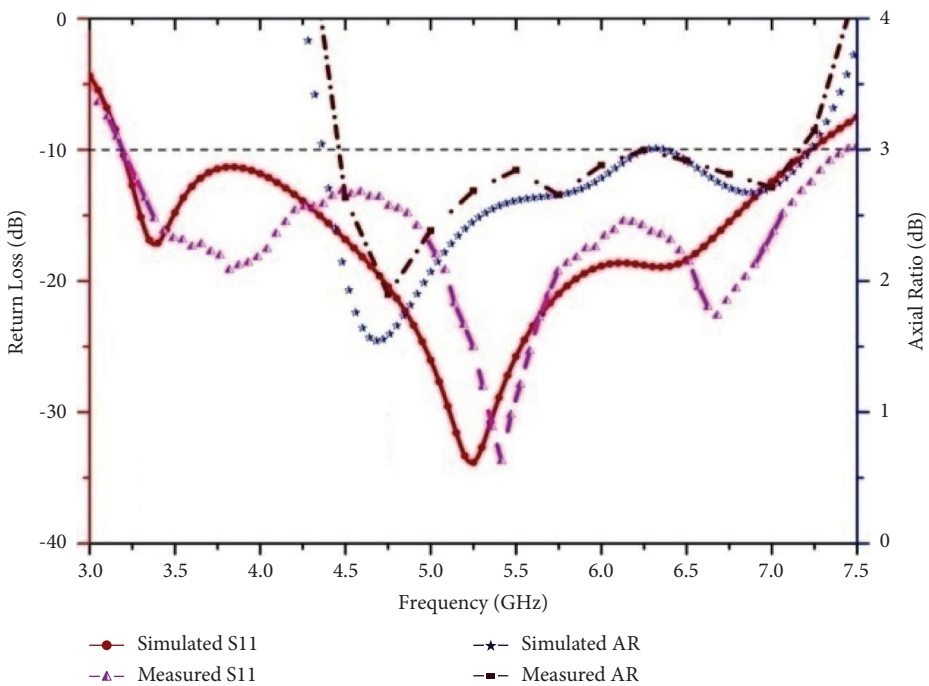

Figure 10: Simulated and measured plots of return loss and axial ratio.

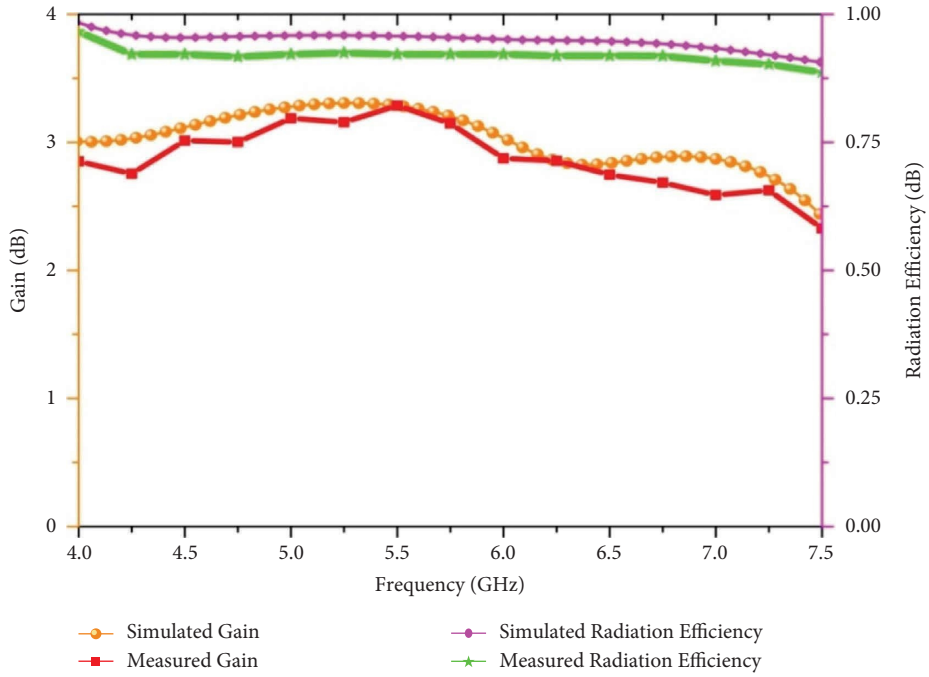

Figure 11: Gain and radiation efficiency.

antenna while increasing its bandwidth and gain. The amazing simplicity of the antenna further indicates its suitability for usage in wireless applications. The specific geometric design and testing results of the suggested antenna are shown in the following sections.

Flexible electronics that are worn on the body stick closely to it. In terms of permittivity and conductivity, wearable gadgets like watches and safety bands are remarkably similar to human tissues, which cause antenna properties to degrade. As a result, it is necessary to evaluate antenna performance in diverse bodily situations. The measurements are carried out using the ANRITSU MS2037C vector network analyzer, and the electromagnetic (EM) computer simulation tool (CST) is used to assess the findings of the antenna simulation (VNA). The measured response of the suggested antennas is fairly consistent with the outcomes of the simulation. The usage of a tiny ground plane, connection losses, and hand manufacturing all contribute to a change in the observed and modelled reflection coefficients. By putting the developed antennas on various human body parts, including the shoulder, wrist, and chest, measurements are made to verify their effectiveness. The on-body status results in a minor change in the reflection coefficients. The high dielectric constant of the different layers of the human body is what causes this frequency detuning. It is possible that the combined impact of the dielectric fluctuation of the cotton shirt and the human body is what causes the impedance mismatch that is noticed at specific frequencies. It should be mentioned that since the human body has a lower volume and mass than other animals, antennas tested on wrists exhibit less detuning and impedance mismatch.

To achieve dual-band behaviour, it is advised to employ a straightforward microstrip patch antenna with a modified ground structure. In comparison to the conventional antennas covered in the preceding sections, the slotted antenna stimulated by a microstrip line has better qualities, such as wider bandwidth, lower conductor loss, and higher isolation between the radiating element and feeding network. By carefully selecting the diameters of the microstrip line and the rectangular slots printed in the ground plane, it is possible to achieve good dual-band impedance bandwidths and sufficient radiation characteristics for use in 2.45 GHz/5.8 GHz RFID operations. In contrast to the antennas previously shown, the recommended structure in this paper not only achieves dual-band operation simultaneously but also has a relatively basic architecture that is easy to fabricate. The antenna characteristics for the proposed multiband antenna are simulated, optimised, and discussed using Computer Simulation Technology Microwave Studio (CST MWS). Using a prototype antenna, the modelling and measurement results have been compared. This study's hypothesis produces a compact, printable structure that might be included in a number of microwave communication systems.

Constructions built on polluted land have been placed here. The antenna ground plane is etched with rectangular holes to increase performance while obtaining the desired frequency bands and an idealised antenna size for a 50 ohm characteristic impedance match.

The recommended antenna has a double-layered metallic design, with one side acting as the substrate and the other as the antenna's ground. With this technique, a conducting strip is directly connected to the microstrip patch's edge. The conductive strip is much thinner than the patch in comparison. The advantage of this feed format is that it allows for a planar structure to be provided by the feed being etched on the same substrate. According to the findings of

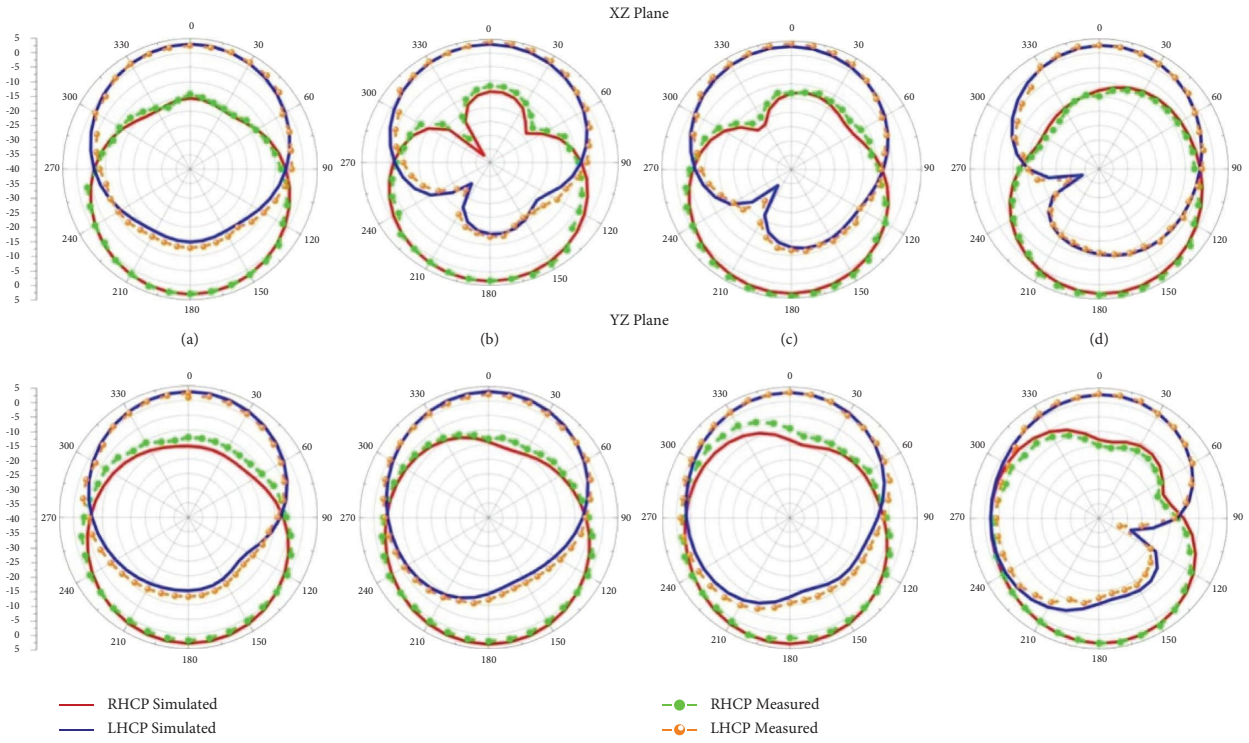

Figure 12: Radiation patterns in the XZ plane and YZ plane for LHCP and RHCP at (a) 4.5 GHz, (b) 5.5 GHz, (c) 5.75 GHz, and (d) 6.5 GHz.

a parametric study, the following elements have an effect on the proposed antenna's bandwidth performance. With all other parameters maintained constant and just one geometrical parameter notably different from the reference design, the antenna is simulated for the parametric study. The parametric analysis depicts the case when the ground plane defect is rectified. There is a clear reduction in bandwidth, and no wireless standard frequency is used. The ground plane's bandwidth is also reduced as it becomes longer. Therefore, size reduction and bandwidth expansion are entirely DGS's responsibility.

The development of the prototype for the investigated antenna enables the verification of simulation results as well as the functionality of the design. The DGS antenna is built using the photolithographic process, a chemical etching technique that produces the required pattern by removing the unwanted metal regions of the metallic layer. The recommended antenna's reflection coefficient demonstrates excellent agreement between modelling and experimental results. The main reasons why the observed and simulated results differ are the effects of soldering at the SMA connection and a little variation in the dielectric permittivity and dissipation factor at high frequencies. In this study, a dual-band, transportable, and compact microstrip antenna for RFID scanners is introduced. This antenna's design is based on a standard DGS structure, and slots have been carved into the ground plane to make fabrication easier. The proposed antenna is a great candidate for the dual-band RFID generation since it also boasts excellent radiation properties and gains in the two operating bands. A tiny *F*-slot antenna that generates dual resonance frequencies and enhances frequency diversity. It is straightforward to get good dual-band functionality for WLAN/Wi-MAX and RFID applications using the *U*-slotted arrangement. The recommended antenna is compact and has a simple layout. It provides broadband impedance matching, a consistent radiation pattern, and tolerable gain characteristics in the RFID and WLAN/Wi-MAX frequency spectrums.

According to earlier research, FR4 printed circuit boards are often utilised to create low-cost antennas with a range of functional capabilities. The antenna's disadvantage is that it is heavy and difficult to bend. Since installing it on curved surfaces would require bending a flexible antenna structure, it cannot be done. Even if certain substrates could be bent, the cost would still be too high. A planar antenna was also made by combining multiple conductive particles with a chemical liquid that resembled printer ink. Silver is the most widely used and accessible conductive powder, with exceptional electrical conductivity. The silver conductive powder is often used in high-frequency or precision operations due to its high cost. It produces conductive printing ink when coupled with a chemical liquid, which is subsequently used to produce a conductive sheet. It is also used in conjunction with pricey specialty printers. However, many academics find it difficult to research and use this method.

WiMax offers a wider communication range than Wi-Fi. Although WiMax applications are more costly than WiFi ones, both are essentially useful. It operates between 2.5 and 3.5 GHz. The radio spectrum is used for nontelecommunication, educational, and commercial uses of radio frequency energy. The industrial, medicinal, and microwave oven settings are where these applications are most often used. Wi-Fi, cordless phones, and Bluetooth devices all operate on ISM frequencies.

Table 2: The antenna's performance is compared to that of previously reported antennas.

Frequencies (GHZ)	Impedance band (GHz) [5–8]	Circularly polarized band (GHz) [9–14]	Dimensions (mm × mm) [5–8]	Antenna design [5–14]	Return loss (dB)	Gain (dB)
5.2	1.85–6.15	1.85–5.9	35 × 35	*S*	−22.58	2.2
7.2	2.75–7.43	2.96–7.26	30 × 30	*L*	−23.58	2.8
7.1	3–7.2	3.1–7.2	33.5 × 37.6	*X*	−24.56	3.2
5.4	3.27–5.89	4.21–5.42	78 × 58	*E*	−25.65	3.5
7.4	3.92–7.52	4.28–7.44	32 × 30	*H*	−26.58	3.6
3.1	1.10–3.19	1.11–2.04	89 × 82	PIFA	−32.45	3.8
2.2	1.84–2.43	1.89–2.43	50 × 50	*V*	−34.68	3.5
6.8	2.37–9	3.22–5.9	38 × 38	*U*	−35.98	4.1
7.23	**3.19–7.23 [*P*]**	**4.37–7.22 [*P*]**	**25 × 25 [*P*]**	***F* [*P*]**	**−36.85**	**4.2**

P means proposed work result.

Unauthorized bands are another term for them. The ISM band's frequencies vary depending on the device; for instance, Bluetooth and Wi-Fi often utilise the 2.4 GHz frequency.

Figure 11 shows a comparison between the prototype antenna's gain and radiation efficiency and simulation findings. In the whole band, a consistent gain of between 2.8 and 3.3 dB is seen. The excellent radiation efficiency covers more than 90% of the band, and the peak gains at 5.28 GHz and 3.28 GHz, respectively, are 3.3 dB anticipated and measured. By contrasting the measured patterns in the XZ plane and YZ plane, as illustrated in Figure, the far-field emission patterns created by the antenna are confirmed. The simulated far-field emission patterns of the antenna are 95.879 at 5.16 GHz and 92.45 at 5.25 GHz. Figures 12(a) through 12(d) illustrate how the RHCP is seen in the $-Z$ direction whereas the LHCP is visible in the $+Z$ direction (d). Figures 12(b) through 12(c) illustrate how the RHCP is seen in the $-Z$ direction, whereas the LHCP is visible in the $+Z$ direction (c). With a few small abnormalities brought on by the use of a poor connection and manufacturing tolerance during measurements, the simulated and real curves quite well match each other. The proposed antenna has compact dimensions and broadband properties when compared to earlier published antennas, as demonstrated in Table 2.

5. Conclusion

A broadband CP monopole antenna fed by the CPW is recommended. Construction and testing of the prototype antenna take place in an anechoic room. A monopole with an *f* shape serves as the radiating element. The ground plane is furnished with twin rectangular slots, a *T*-Type slot, and corner-truncated square slots to produce broad circular polarisation, a steady gain, and excellent radiation efficiency. Measurement results, such as return loss values ranging from 3.19 to 7.4 GHz with 79.5% and axial ratio values ranging from 4.52 to 7.15 GHz with 45.07%, were in very good agreement with the modelling results. The CP band reaches a peak gain of 3.3 dBic and a radiation efficiency of 95%. The performance of small, *F*-shaped flexible antennas is assessed for wearable applications. The usage of the suggested antennas for wearable systems/devices is highly supported by the experimental findings. The suggested antennas have superior gain and efficiency, lower SAR values, excellent path loss characteristics, and fewer group delay changes. They also have a bandwidth of >7.5 GHz. The created flexible antennas may be easily included in cotton clothing and are advised for use in security, medical, sports, and rescue applications.

The recommended CP antenna is suitable for WLAN and WiMAX applications and has constant radiation characteristics. It was shown that the suggested design was very flexible and that bending did not significantly affect the performance of the suggested antennas. In addition, the present version does not include measurable findings since the manufacturing facilities are not readily available. To create a multiband, an inverted *F*-shaped slot is added to the patch, and a microstrip line is also included for feeding. Better return loss, bandwidth, VSWR, gain, and directivity need different parameter tuning. There are no resonant frequencies that have return losses greater than −10 dB. As shown, the results of the simulations indicate that the suggested antenna will function more effectively for applications in the *S*, *C*, *X*, and Ku bands. The developed antenna is clearly superior to the others when compared to earlier research. The antenna's justified return loss, VSWR, and positive gain make it suitable for all of the aforementioned applications. The antenna would next be constructed, and the results would be tested. It is important to take into account the antenna's limited strength and bandwidth.

Data Availability

No data were used to support this study.

Conflicts of Interest

The authors declare that they have no conflicts of interest.

Authors' Contributions

A. Gokula Chandar, R. Nagarajan, Mahtab Mashuq Tonmoy, and Parameswari Subbian were in charge of design, writing, editing, and implementation; and S. Kannadhasan was in charge of design, writing, editing, implementation, and results.

References

[1] S. Kumar, K. W. Kim, H. C. Choi et al., "A low profile circularly polarized UWB antenna with integrated GSM band for wireless communication," *AEU - International Journal of Electronics and Communications*, vol. 93, pp. 224–232, 2018.

[2] U. Banerjee, A. Karmakar, A. Saha, and P. Chakraborty, "A CPW-fed compact monopole antenna with defected ground structure and modified parasitic hilbert strip having wideband circular polarization," *AEU - International Journal of Electronics and Communications*, vol. 110, Article ID 152831, 2019.

[3] K. U. Sam and P. Abdulla, "Truncated circular microstrip ultra wideband antenna exhibiting wideband circular polarization," *Progress in Electromagnetics Research C*, vol. 99, pp. 111–122, 2020.

[4] H. Zhai, D. Yang, L. Xi, and D. Feng, "A new CPW-fed broadband circularly polarized printed monopole antenna for UWB application," *Microwave and Optical Technology Letters*, vol. 60, no. 2, pp. 364–369, 2018.

[5] Z. Li, X. Zhu, and C. Yin, "CPW-fed ultra-wideband slot antenna with broadband dual circular polarization," *AEU - International Journal of Electronics and Communications*, vol. 98, pp. 191–198, 2019.

[6] C. Zhou, G. Wang, Y. Wang, B. Zong, and J. Ma, "CPW-fed dual-band linearly and circularly polarized antenna employing novel composite right/left-handed transmission-line," *IEEE Antennas and Wireless Propagation Letters*, vol. 12, pp. 1073–1076, 2013.

[7] H. Alsariera, Z. Zakaria, A. Awang Md Isa et al., "A compact broadband coplanar waveguide fed circularly polarized printed monopole antenna with asymmetric modified ground plane," *International Journal of RF and Microwave Computer-Aided Engineering*, vol. 30, no. 7, Article ID e22205, 2020.

[8] K. Oteng Gyasi, G. Wen, D. Inserra et al., "A compact broadband circularly polarized slot antenna with two linked rectangular slots and an inverted-F feed line," *IEEE Transactions on Antennas and Propagation*, vol. 66, no. 12, pp. 7374–7377, 2018.

[9] U. Ullah, S. Koziel, and I. B. Mabrouk, "A simple-topology compact broadband circularly polarized antenna with unidirectional radiation pattern," *IEEE Antennas and Wireless Propagation Letters*, vol. 18, no. 12, pp. 2612–2616, 2019.

[10] B. R. Behera, P. Srikanth, P. R. Meher, and S. K. Mishra, "A compact broadband circularly polarized printed monopole antenna using twin parasitic conducting strips and rectangular metasurface for RF energy harvesting application," *AEU - International Journal of Electronics and Communications*, vol. 120, Article ID 153233, 2020.

[11] H. Zhang, Y.-C. Jiao, L. Lu, and C. Zhang, "Broadband circularly polarized square-ring-loaded slot antenna with flat gains," *IEEE Antennas and Wireless Propagation Letters*, vol. 16, pp. 29–32, 2017.

[12] S. Mohammadi, J. Nourinia, C. Ghobadi, J. Pourahmadazar, and M. Shokri, "Compact broadband circularly polarized slot antenna using two linked elliptical slots for C-band applications," *IEEE Antennas and Wireless Propagation Letters*, vol. 12, pp. 1094–1097, 2013.

[13] H.-D. Chen, C. Y. D. Sim, and S. H. Kuo, "Compact broadband dual coupling-feed circularly polarized RFID microstrip tag antenna mountable on metallic surface," *IEEE Transactions on Antennas and Propagation*, vol. 60, no. 12, pp. 5571–5577, 2012.

[14] B. Xu, S. Zhang, Y. Liu, J. Hu, and S. He, "Compact broadband circularly polarised slot antenna for universal UHF RFID readers," *Electronics Letters*, vol. 51, no. 11, pp. 808-809, 2015.

[15] H. Tang, K. Wang, R. Wu, and C. Yu, "Compact broadband CP monopole antenna with tilted branch," *Electronics Letters*, vol. 52, no. 21, pp. 1739-1740, 2016.

[16] W. Abdelrahim and Q. Feng, "Compact broadband dual-band circularly polarised antenna for universal UHF RFID handheld reader and GPS applications," *IET Microwaves, Antennas & Propagation*, vol. 13, no. 10, pp. 1664–1670, 2019.

[17] J. Li, H. Liu, S. Zhang, Y. Zhang, and S. He, "Compact broadband circularly-polarised antenna with a backed cavity for UHF RFID applications," *IET Microwaves, Antennas & Propagation*, vol. 13, no. 6, pp. 789–795, 2019.

[18] Y. Kumar, R. K. Gangwar, and B. K. Kanaujia, "Compact broadband circularly polarized hook-shaped microstrip antenna with DGS plane," *International Journal of RF and Microwave Computer-Aided Engineering*, vol. 28, no. 6, Article ID e21275, 2018.

[19] S. Kannadhasan and R. Nagarajan, "Development of an H-shaped antenna with FR4 for 1-10GHz wireless communications," *Textile Research Journal*, vol. 91, no. 15-16, pp. 1687–1697, 2021.

[20] S. Kannadhasan and R. Nagarajan, "Performance improvement of h-shaped antenna with zener diode for textile applications," *The Journal of the Textile Institute*, vol. 113, no. 8, 2021.

[21] S. Ullah, I. Ahmad, Y. Raheem, S. Ullah, T. Ahmad, and U. Habib, "Hexagonal shaped CPW feed based frequency reconfigurable antenna for WLAN and sub-6 GHz 5G applications," in *Proceedings of the 2020 International Conference on Emerging Trends in Smart Technologies (ICETST)*, pp. 1–4, Piscataway, NJ, USA, March 2020.

[22] U. Ali, S. Ullah, J. Khan et al., "Design and SAR analysis of wearable antenna on various parts of human body, using conventional and artificial ground planes," *Journal of Electrical Engineering and Technology*, vol. 12, no. 1, pp. 317–328, 2017.

[23] F. Faisal, A. Ahmad, U. Ali, S. Ullah, and K. Ullah, "Performance analysis of a 2.4 GHz planar antenna using different types of wearable artificial ground planes," in *Proceedings of the 12th International Conference on High-Capacity Optical Networks and Enabling/Emerging Technologies (HONET)*, pp. 1–5, Islamabad, Pakistan, December 2015.

[24] P. J. Soh, F. N. Giman, M. F. Jamlos, H. Lago, and A. A. Al-Hadi, "C-slotted dual band textile antenna for WBAN applications," in *Proceedings of the URSI Asia-Pacific Radio Science Conference (URSI AP-RASC)*, pp. 1621–1624, New Delhi, India, March 2019.

[25] F. Faisal and H. Yoo, "A miniaturized novel-shaped ual-band antenna for implantable applications," *IEEE Transactions on Antennas and Propagation*, vol. 67, no. 2, pp. 774–783, 2019.

[26] T. S. Bird, "Definition and misuse of return loss report of the transactions editor in chief," *IEEE Antennas and Propagation Magazine*, vol. 51, no. 2, pp. 166-167, 2009.

[27] U. Patel, M. Parekh, A. Desai, and T. Upadhyaya, "Wide slot tri-band antenna for wireless local area network/world-wide interoperability for microwave access applications," *International Journal of Communication Systems*, vol. 34, no. 12, Article ID e4897, 2021.

[28] R. Patel, T. Upadhyaya, and A. Desai, "Capacitive couplings compact antenna for LTE/WiMAX/WLAN application," *Microwave and Optical Technology Letters*, vol. 60, no. 12, pp. 2977–2983, 2018.

[29] H. Patel and T. K. Upadhyaya, "Printed multiband monopole antenna for smart energy meter/WLAN/WiMAX applications," *Progress in Electromagnetics Research M*, vol. 89, pp. 43–51, 2020.